Journal of Molecular Liquids 219 (2016) 592–598

Contents lists available at ScienceDirect

Journal of Molecular Liquids

journal homepage: www.elsevier.com/locate/molliq

Water-soluble inclusion complexes of *trans*-polydatin by cyclodextrin complexation: Preparation, characterization and bioactivity evaluation

Jian-Qiang Zhang [a], Kun-Ming Jiang [a], Xiao-Guang Xie [a,*], Yi Jin [a,*], Jun Lin [a,b,**]

[a] Key Laboratory of Medicinal Chemistry for Natural Resource (Yunnan University), Ministry Education, School of Chemical Science and Technology, Yunnan University, Kunming 650091, PR China
[b] Advanced Analysis and Measurement Center, Yunnan University, Kunming 650091, PR China

ARTICLE INFO

Article history:
Received 30 September 2015
Received in revised form 9 February 2016
Accepted 19 March 2016
Available online xxxx

Keywords:
trans-Polydatin
Cyclodextrins
Characterization
Inclusion complex
In vitro activity

ABSTRACT

The inclusion complexes of *trans*-polydatin (PD) with β-CD and γ-CD were prepared. The inclusion complexation behavior, characterization and interactions of PD with CDs were investigated in both the solution and the solid state by means of UV–vis, ESI-MS, NMR, FT-IR, XRD, SEM, TG and DSC. All of the characterization information demonstrated the formation of PD/CDs inclusion complex, and the PD/CDs inclusion complexes exhibited different spectroscopic features and properties from PD. The 1:1 stoichiometry of the complexes was visually proven with the ESI-MS experiment and Job's method. Meanwhile, it was the phenyl group (a and b rings) of the PD molecule that were included in the CDs cavity from the wide side. Moreover, the water solubility of PD/CDs was significantly improved from 0.161 mg/mL to 7.21 mg/mL (PD/β-CD) and 12.02 mg/mL (PD/γ-CD). Consequently, the bioavailability of PD/CDs inclusion complexes were effectively improved over free PD in vitro. The present study provides useful information for the potential application of complexation with PD, a naturally occurring hydrophobic polyphenolic compounds herbal medicine.

1. Introduction

In recent years, several scientific studies have attracted considerable attention to the fact that moderate but regular red wine consumption has beneficial effects on human health [1]. Polyphenolic compounds, which are present in the skin of grapes and in red wine, are proposed to be responsible for these activities, particularly stilbene compounds, such as polydatin. It also named piceid (*trans*-polydatin, 3,4′,5-trihydroxystilbene-3-β-*D*-glucoside), the chemical structure of which is shown in Fig. 1**A**, is one of the main effective elements of *P. cuspidatum*. Polydatin injection which the main component is PD, the traditional Chinese medicine, is the first to submit an application for clinical research in the United States as a kind of innovative drugs. Previously, pharmacological studies and clinical practice have demonstrated that PD has a number of biological functions, such as against shock [2–4], ischemia/reperfusion injury [5,6], congestive heart failure [7], endometriosis [8] and antitumor [9–11]. However, the use of PD as a natural herbal medicine is greatly limited by its low water solubility and bioavailability. Therefore, various formulation techniques are applied to enhance the aqueous solubility of poorly water-soluble drugs, including the formulation of amorphous solid forms, nanoparticles, microemulsions, solid dispersions, melt extrusion, salt formation and the formation of water-soluble complexes [12,13]. The search for an efficient and nontoxic carrier for PD has become important in order to further its clinical applications.

This problem may be solved by the formation of inclusion complexes with cyclodextrin (CD), which usually increases the stability, solubility, dissolution rate and bioavailability [14–16]. Cyclodextrins are a family of molecules comprised of several glucopyranoses bound together to form a ring [17]. Among many types of cyclodextrins occurring in nature, β- and γ-cyclodextrin are torus-shaped oligosaccharide containing seven or eight glucose units (Fig. 1B) with a hydrophilic outer surface and a lipophilic inner cavity that can accommodate a wide variety of lipophilic drugs, forming the inclusion complexes. Our group has reported that many inclusion complexes of CDs with natural products significantly enhanced the water solubility and bioavailability of the products [18–21].

PD has attracted considerable interest for chemists due to its biological activities. Recent, the group of He [22] and Liang [23] reported the inclusion complex of PD with HP-β-CD and 6-O-α-maltosyl-β-CD, their physicochemical characteristics has been studied and characterized. To develop different PD/CDs and their applications, the complexes of PD with β- and γ-CD were prepared using a simple freeze-drying method in the present study. UV–vis spectroscopy was used to evaluate the formation of PD/CDs complexes in aqueous solutions, Drug/CDs interactions in the solution were investigated using a phase solubility analysis. The interactions in the solid state were characterized using

* Corresponding authors.
** Correspondence to: J. Lin, Key Laboratory of Medicinal Chemistry for Natural Resource (Yunnan University), Ministry Education, School of Chemical Science and Technology, Yunnan University, Kunming 650091, PR China.
E-mail addresses: xgxie@ynu.edu.cn (X.-G. Xie), jinyi@ynu.edu.cn (Y. Jin), linjun@ynu.edu.cn (J. Lin).

http://dx.doi.org/10.1016/j.molliq.2016.03.054
0167-7322/

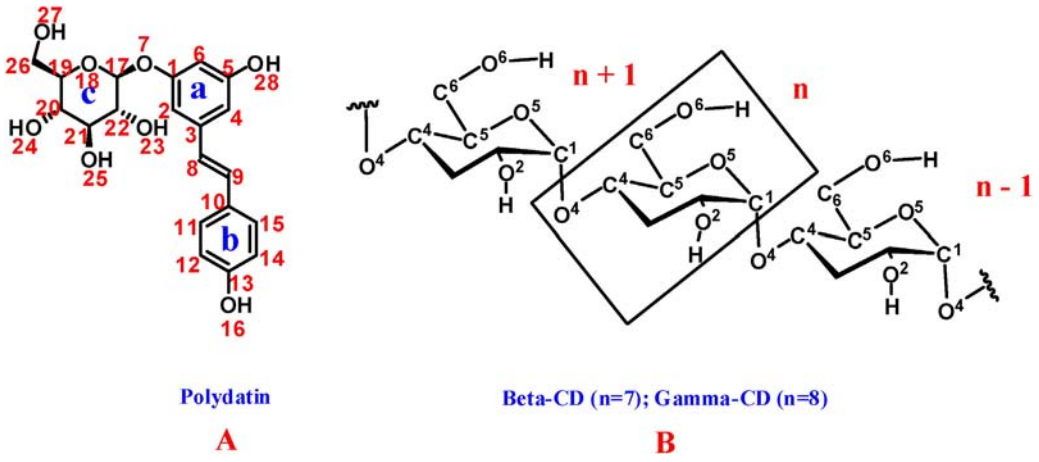

Fig. 1. Chemical structure of polydatin (A) and β-, γ-CD (B).

NMR, FT-IR, XRD, SEM, TG and DSC, aiming to verify the formation of the inclusion complex. The 1:1 stoichiometry was confirmed by the continuous variation Job's method, and ESI-MS [24,25] examinations gave direct evidence for the 1:1 binding model. Finally, the inhibitory effects of PD/CDs on cell growth were evaluated to prove the retaining bioactivity of free PD.

2. Materials and methods

2.1. Materials

Polydatin (FW = 390.13, purity > 99%) was obtained from Sigma-Aldrich (Dorset, UK). β-CD (FW = 1135, purity > 99%) and γ-CD (FW = 1297, purity > 99%) were purchased from *Adamas Reagent Co. Ltd.* and used without further purification. Other reagents and chemicals were of analytical reagent grade. All experiments were carried out using ultrapure water.

2.2. Preparation of the inclusion complexes and physical mixtures

The 1:1 M ratio of the PD/CDs inclusion complexes was prepared using the freeze-drying method [26]. Accurately weighed amounts of β- and γ-CD were dissolved in ultrapure water. Subsequently, the solution of PD in ethanol was added slowly to the aqueous CDs solution. The resulting suspension was stirred at room temperature for 48 h. It was then filtered through a 0.22 μm membrane filter before being lyophilized with a freeze dryer (Alpha 2–4, Christ) to obtain the solid complexes. The physical mixtures used to test for possible inclusion were prepared by mixing the powders at a 1:1 M ratio of PD and CDs in an agate mortar.

2.3. Stoichiometry determination: Job's method and phase-solubility studies

The UV–vis absorption spectra of PD, CDs and the inclusion complexes were recorded using a UV-2401 spectrophotometer (Shimadzu, Tokyo, Japan) in the range of 200–500 nm. The stoichiometry of the inclusion complex was determined using the continuous variation Job's method [27,28]. To experimentally implement Job's method, equimolar 1.64×10^{-5} M solutions of PD and CDs were mixed to a standard volume containing a fixed total concentration of the species. In the solutions, the R (R = [PD]/([PD] + [CDs]), [PD] + [CDs] = 3.28×10^{-5} M) is systematically varied from large to small. The maximum amount of the complex PD should occur at the stoichiometric ratio from 0.0 to 1.0.

2.4. Inclusion complex characterization

2.4.1. NMR spectroscopy

1H NMR and ROESY spectra were obtained on an Ascend 500 MHz NMR spectrometer (Bruker, Switzerland). β-CD and γ-CD complexes and PD were dissolved in D_2O (or DMSO-d_6) and DMSO-d_6 respectively. Chemical shifts were reported in ppm with tetramethylsilane (TMS) as the internal standard.

2.4.2. Fourier-transform infrared spectroscopy (FT-IR)

FT-IR spectra were recorded on the Fourier transform infrared spectrometer (Nicolet 6700, Thermo Fisher Scientific, Waltham, MA) according to the KBr disk technique. Samples were prepared as KBr disks with 1 mg of complex in 100 mg of KBr. The FTIR measurements were performed in the scanning range of 4000–400 cm^{-1} at ambient temperature.

2.4.3. Powder X-ray diffractometry (XRD)

X-ray powder diffraction patterns [29] were performed on a Philips X'Pert Pro diffractometer using Ni-filtered and Cu Kα radiation (45 kV, 35 mA). The scanning rate employed was 0.15°/min in a diffraction angle (2θ) range of 3°–50°.

2.4.4. Scanning electron microscopy (SEM)

Scanning electron microscopy (SEM) was used to evaluate the morphology of PD, β-CD, and γ-CD inclusion complexes and the physical mixture. All samples were made electrically conductive by coating them with a thin layer of gold before the examination using a JEOL JSM-7500F scanning electron microscope operated at 5.0 kV.

2.4.5. Thermogravimetry

Differential scanning calorimetry (DSC) and thermogravimetric (TG) measurements were conducted on a 2960 SDT V3·0F instrument and NETZSCH STA 449F3, respectively, and 3–3.5 mg of each sample was heated at a rate of 10 °C/min from room temperature to 400 °C under dynamic nitrogen atmosphere and at a flow rate of 70 mL/min.

2.4.6. Mass spectrometry

The complexes of PD with CDs were prepared by the addition of an equimolar portion of the PD to an aliquot of CDs in an aqueous solution (5.5 mmol/L). Then, the whole solution was shaken for 48 h to mix it effectively before introducing it to the mass spectrometer. Electrospray ionization mass spectrometry (ESI-MS) experiments were performed using an Agilent 1100 LCF MSD TOF mass spectrometer (Agilent, USA) equipped with an electrospray source. The sample was introduced via a syringe pump at a flow rate of 3 μL/min. High flow rate nitrogen gas

was employed as the nebulizing gas, as well as the drying gas, to aid desolation. After optimization of the MS parameters, the spray voltage was set to 4.0 kV in the positive mode and the heated metal capillary temperature was set at 300 °C. The fragmentor and skimmer voltages were set at 250 and 75 V, respectively. The mass scale was calibrated by using the standard calibration procedure and compounds provided by the manufacturer.

2.5. Cell growth inhibition assay

The cell growth inhibition on human lung adenocarcinoma cell (A549), human cervical cancer (Hela), human ovarian cancer cell (SKOV-3) and human breast adenocarcinoma (HepG2) cell lines were determined by an MTT assay [30] as described previously. In this assay, the increase or decrease in the number of viable cells is linearly correlated with the mitochondrial activity, highlighted by the conversion of the tetrazolium salt (MTT) into formazan crystals, which can be solubilized and spectrophotometrically quantified. First, cells were grown in 96-well plates at 5000 cells per well in a final volume of 200 μL of culture medium per well. Then, the cells were cultured in an incubator (5% CO_2, 37 °C) until the cells reached 70–80% confluency. After culturing the cells in an incubator for 48 h, 20 μL of MTT solution was added to each well and incubated for 2 h. The culture medium was discarded, and 200 μL of DMSO were added to each well. The solution was then swirled gently and left in the dark for 10 min. The absorbance in each well was measured at 570 nm in a microtiter plate reader. The cell viability in treated cells was expressed as the amount of dye reduction relative to that of the untreated control cells.

3. Results and discussion

3.1. NMR spectra analysis

1H NMR spectra are some of the most direct evidence for the formation of the inclusion complex [31–33]. If a guest molecule is incorporated into the CDs cavity, the screening constants of the CDs protons inside the cavity (H-3 and H-5) should be sensitive to the changed environment, but that of the outside protons (H-1, H-2, and H-4) should not. This should result in chemical shift changes of the inside protons [20]. The 1H chemical shifts of CDs were determined through the 1H NMR spectra of CDs and PD, as well as their complexes. These results are shown in Table 1.

The chemical shifts for the PD (Fig. 2A(a)) are as follows: 1H NMR (500 MHz, DMSO-d_6) δ 9.60 (s, H-16 of PD), 9.47 (s, H-28 of PD), 7.45–7.39 (m, H-11 and H-15 of PD), 7.05 (d, J = 16.3 Hz, H-8 of PD), 6.89 (d, J = 16.3 Hz, H-9 of PD), 6.81–6.73 (m, H-2, H-12 and H-14 of PD), 6.59 (t, J = 1.7 Hz, H-6 of PD), 6.36 (t, J = 2.2 Hz, H-4 of PD), 5.31 (d, J = 5.1 Hz, H-17 of PD), 5.12 (d, J = 4.8 Hz, H-24 of PD), 5.05 (d, J = 5.3 Hz, H-23 of PD), 4.82 (d, J = 7.6 Hz, H-27 of PD), 4.66 (t, J = 5.7 Hz, H-25 of PD), 3.75 (ddd, J = 11.8, 5.3, 2.1 Hz, H-22 of PD), 3.51 (dt, J = 11.9, 6.1 Hz, H-19 of PD), 3.38–3.14 (m, H-20, H-21 and H-26 of PD). The Δδ in the 1H chemical shift for PD and CDs originating from the complexation phenomena was calculated by applying Eq. (1) as follows:

$$\Delta\delta = \delta_{complex} - \delta_{free} \quad (1)$$

1H NMR spectra (Fig. 2A) of the complexes showed the proton peaks of both CDs and PD. Furthermore, several 1H chemical shifts of CDs were changed. This confirmed that the complexes were formed. Table 1 showed that the chemical shift of outside protons H-1 and H-6 had a little variation before and after forming the complex. While significant chemical shift changes were exhibited by H-5 and H-3 protons in the inner surface of CD with an up-field shift from −0.110 ppm to −0.150 ppm. It is noteworthy that the chemical shift variation for H-3 was smaller than H-5 after resulting inclusion complex. Since both H-3 and H-5 protons from each sugar unit are located in the internal cavity of CD, we can propose from the 1H NMR data that PD was included in the CD cavity.

Two-dimensional (2D) NMR [34] provides the most direct evidence for the spatial proximity between the host and guest atoms following the observation of intermolecular dipolar cross-correlations. Two protons closely located in space can produce a Nuclear Overhauser Effect (NOE) cross-correlation in NOE spectroscopy (NOESY) or rotating-frame NOE spectroscopy (ROESY) [35]. These NOE cross-peaks between the protons of the host and guest molecules point to spatial contacts within 0.4 nm. 2D ROESY off resonance was used to study the inclusion of PD with β-CD and γ-CD.

Fig. 2B shows a section of the contour plot of the ROESY spectrum of the PD/γ-CD complex. First of all, it should be noted that the ROESY spectrum showed a correlation between H-4, H-6, H-8, H-9, H-11, H-12, H-14 and H-15 of PD and H-3 and H-5 of γ-CD, indicating that the phenyl group (a and b rings) of PD were incorporated inside the γ-CD cavity. These observations were not surprising since the most probable mode of binding in the CD inclusion complexes involved the incorporation of the less polar moiety of the guest inside the cavity. We also found NOE cross peaks with the inner CD protons, and to a larger extent with H-6, demonstrating the PD binding with outside contribution. 2D NMR results were in good agreement with results obtained from the 1H chemical shifts analysis. It was also shown that PD should be included in the β-CD cavity from the wide side (see Supplementary Data).

3.2. Scanning electron microscopy

Scanning electron microscopy (SEM) [36,37] is a qualitative method used to visualize the surface structure of raw materials or the prepared products. The SEM images of the PD, β-CD, and PD/β-CD inclusion complex, as well as their physical mixtures, were illustrated in Fig. 3A. Pure PD existed in a needle-like crystal with many different sizes (Fig. 3A (a)), whereas β-CD was observed as rod-like crystals (Fig. 3A (b)). In the physical mixture, the characteristic β-CD microspheres, which were mixed with PD crystals or adhered to their surface, were clearly observed (Fig. 3A (d)). However, the PD/β-CD inclusion complex appeared in the form of irregular block-like particles (Fig. 3A (c)) in which the original morphology of both components disappeared, confirming the formation of the inclusion complex of PD and β-CD. These changes can be taken as proof of the formation of new inclusion complexes by molecular encapsulation (SEM of γ-CD and inclusion complex, see the Supplementary Data).

3.3. Stoichiometry determination: Job's method

The standard curve was performed using a UV–vis spectrophotometer at 317 nm, which was prepared using the concentration (C, mM) as the x-coordinate and the absorbance (A) as the y-coordinate. The standard curve of PD can be expressed as $A = 29.1199C + 3.8 \times 10^{-3}$ (R^2 = 0.9947).

Table 1
Chemical shifts of ^{1}H NMR of CD protons in the presence and absence of PD.

Protons	Chemical shift (ppm)					
	$\delta_{\beta\text{-CD}}$	$\delta_{PD/\beta\text{-CD}}$	$\Delta\delta_{\gamma}$	$\delta_{\gamma\text{-CD}}$	$\delta_{PD/\gamma\text{-CD}}$	$\Delta\delta_{\gamma}$
H-1	4.916	4.865	−0.051	4.977	4.925	−0.052
H-2	3.495	3.440	−0.055	3.526	3.475	−0.051
H-3	3.815	3.705	−0.110	3.864	3.715	−0.149
H-4	3.434	3.395	−0.039	3.462	3.426	−0.036
H-5	3.707	3.565	−0.142	3.765	3.615	−0.150
H-6	3.720	3.632	−0.088	3.786	3.652	−0.134

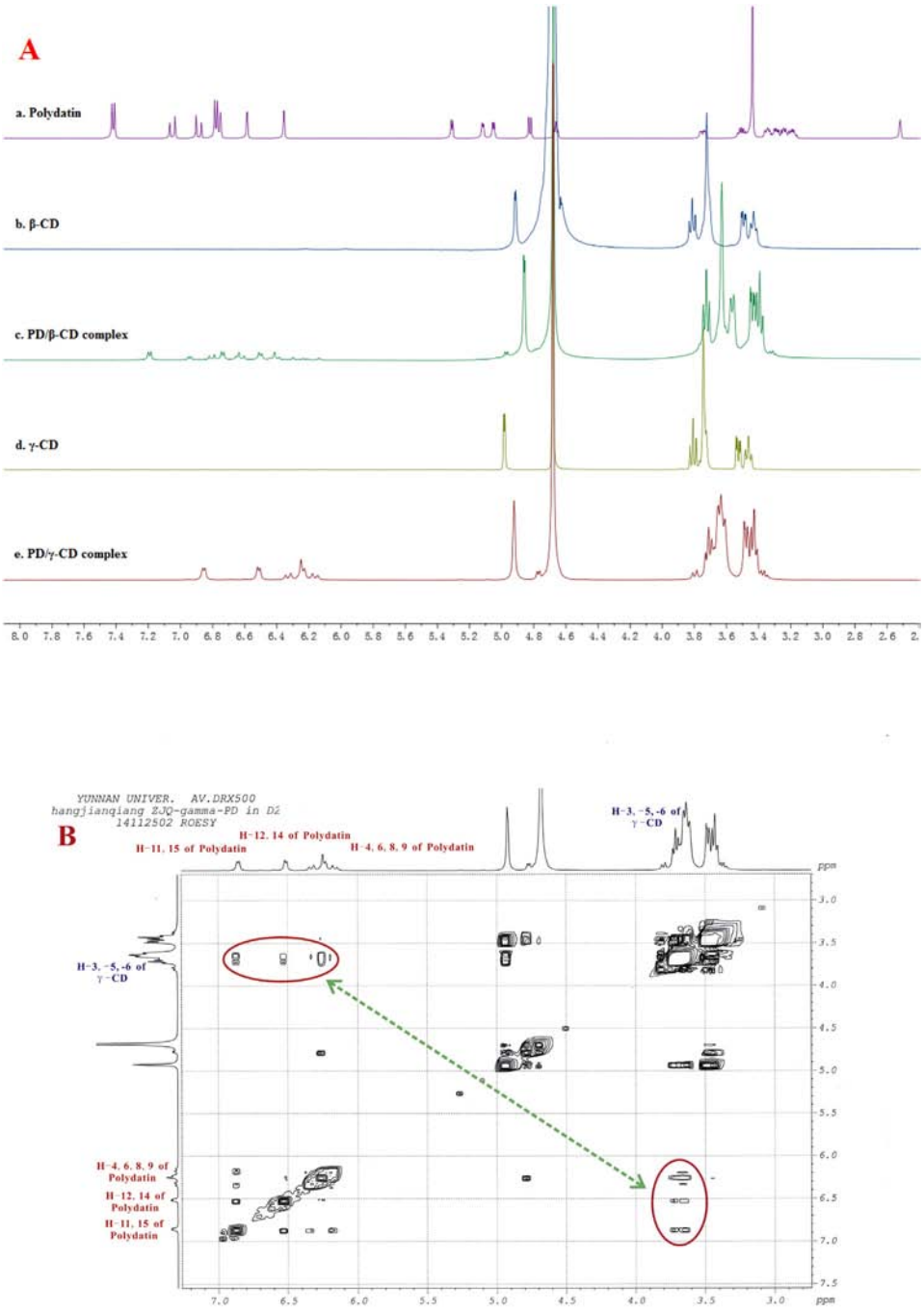

Fig. 2. (A): 1H NMR spectra of PD in the absence and presence of β-CD and γ-CD in D_2O at 25 °C, respectively; (B): ROESY spectrum of PD/γ-CD in D_2O.

The stoichiometry of complex formation between PD and CD was also determined using *Job's Method*. The Job's plot is shown in Fig. 3B. As shown in the Job's plot, the maximum peak was obtained at R = 0.5, indicating the formation of 1:1 inclusion complexes between PD and β-CD or γ-CD, in agreement with the phase solubility study.

3.4. FTIR spectroscopy

FTIR is a useful technique for confirming the formation of the inclusion complex [38,39]. Moreover, the modifications in the FTIR spectra are typical of the solid-state complexes, due to the loss of the vibrating and bending of the guest molecule upon complexation. FT-IR spectra of PD, β-CD and γ-CD inclusion complexes and the physical mixture were recorded at room temperature in a spectral region between 4000 and 400 cm^{-1}, as shown in Fig. 4A.

We can observe that the FTIR spectra of inclusion complexes and free CDs were very similar (Fig. 4A (b, c, e, f)). Moreover, bands of PD were almost completely obscured by very intense and broad CD bands. In both PD/β-CD and PD/γ-CD inclusion complex spectra, PD absorption peaks at 3473, 3362, 1596, 1511, 1447, 1321, 1249, 1172, 1079 and 834 cm^{-1} were no longer able to be identified. However, the bands at 1249 and 834 cm^{-1}, which are respectively attributed to υ (C—O—C) and δ (C—H) of para-substituted phenyl group of PD, were detected with a very slight shift and a decreased intensity. Furthermore, we could see that the band of the centroid of both complexes was shifted in the range of the OH vibrations towards lower frequencies compared

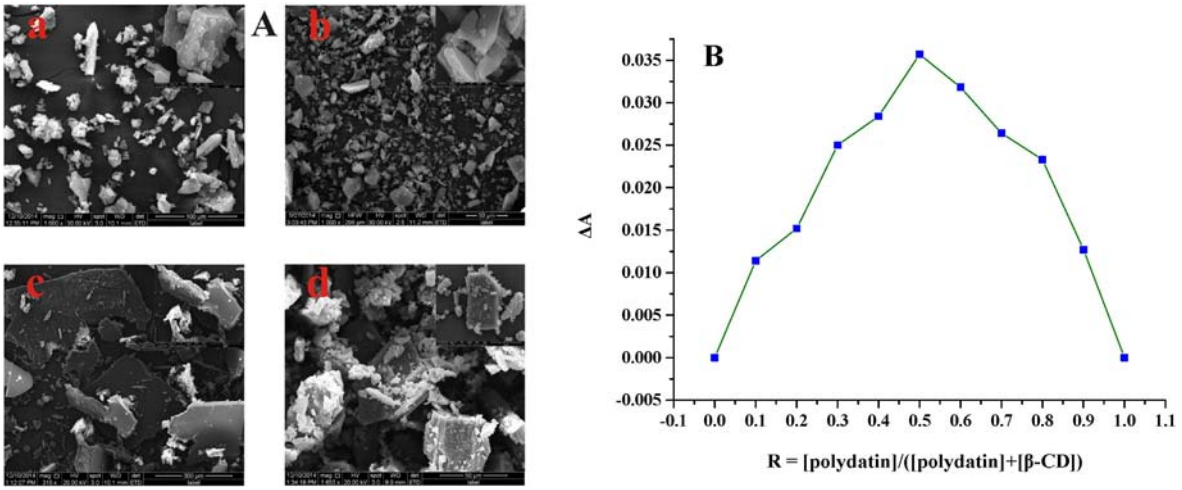

Fig. 3. (A) SEM: (a) PD, (b) β-CD, (c) PD/β-CD inclusion complex, (d) PD/β-CD physical mixture. (B) Job's continuous variation plot of the PD/β-CD complex.

to the position of the similar band in the β-CD and γ-CD spectra, respectively. This may be related to a change of hydration bond structure due to the formation of intramolecular hydrogen bonds between PD and CDs. In addition, we noticed that no new peaks were observed, proving that no new chemical bonds were created. The spectrum of the physical mixture was equivalent to the simple combination of PD and CDs. Some characteristic absorption peaks of PD at 3493, 1956, 1447, 1249, 1079, and 835 cm^{-1} were easy to observe (Fig. 4A (d, g)), suggesting that the natural structure of PD still existed without any interactions with β-CD and γ-CD. All of these results provided further evidence of the inclusion of PD in the hydrophobic cavity of β-CD and γ-CD. The overall FTIR results confirmed that inclusion complex was formed and the benzene ring was included in the CD nano-cavity, which was in accordance with the NMR results.

3.5. DSC analysis

The DSC curves of pure PD, CDs and solid inclusion complexes are shown in Fig. 4B. The thermogram of PD (Fig. 4B (a)) shows a sharp endothermic peak (228 °C) [40], corresponding to the melting point of PD. The thermal profile of CDs (Fig. 4B (b, d)) shows a broad endothermic peak at 108 °C and 79 °C, corresponding to its dehydration of β-CD and γ-CD. The decomposition was 308 °C and 323 °C, respectively. However, the DSC curves of the PD/CDs complexes changed to new peaks, corresponding to free PD with endothermic peaks at about 228 °C. Then, it disappeared, coinciding with the appearance of the endothermic peak at 80 °C and 79 °C in the case of the PD/β-CD and PD/γ-CD (Fig. 4B (c, e)) complexes, respectively. The inclusion compound formation could be due to the disappearance of the PD melting point, and

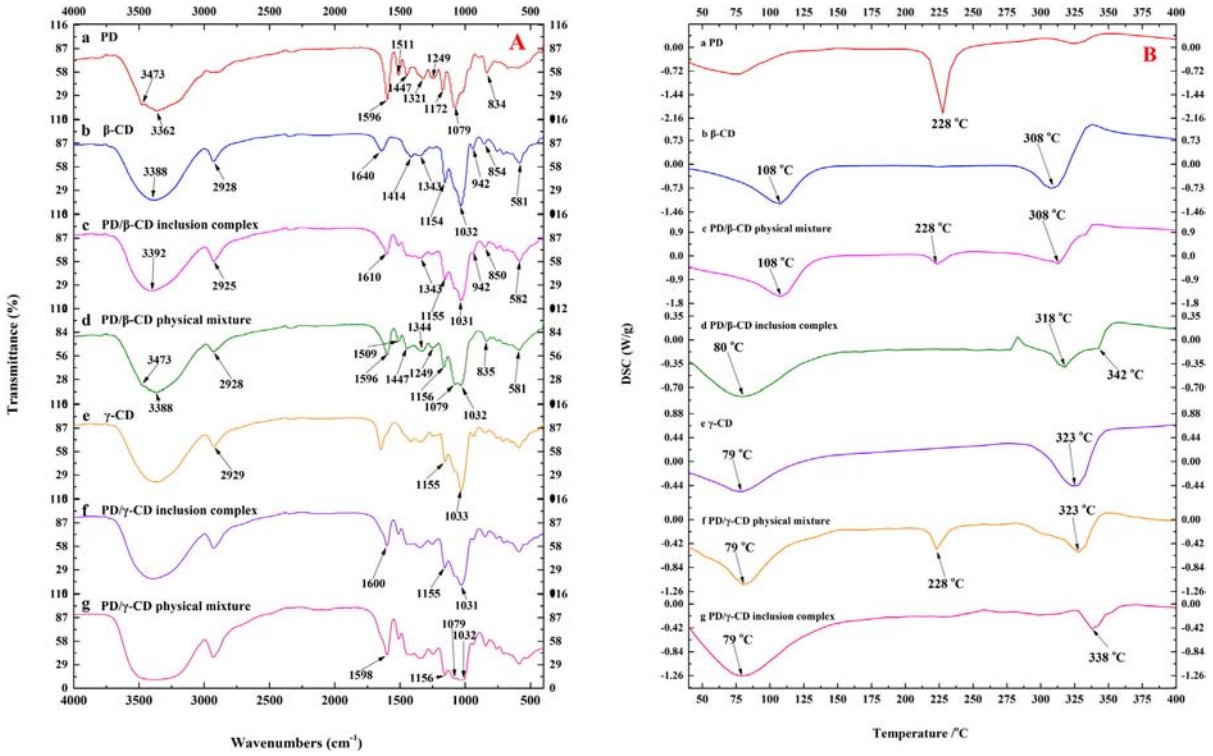

Fig. 4. (A) FTIR spectra and (B) DSC patterns: (a) PD, (b) β-CD, (c) PD/β-CD inclusion complex, (d) PD/β-CD physical mixture, (e)γ-CD, (f) PD/γ-CD inclusion complex and (g) PD/γ-CD physical mixture.

Table 2
In vitro cytotoxic activities of PD and PD/CD inclusion complex.

Cell lines	Compounds	IC_{50} (μM)	(±)SD
A549	PD/β-CD complex	19.03	0.31
	PD/γ-CD complex	17.16	0.42
	PD	27.36	0.36
Hela	PD/β-CD complex	31.12	0.25
	PD/γ-CD complex	25.09	0.33
	PD	44.96	0.49
HepG2	PD/β-CD complex	30.23	0.16
	PD/γ-CD complex	20.06	0.38
	PD	35.56	0.46
SKOV-3	PD/β-CD complex	30.96	0.52
	PD/γ-CD complex	22.53	0.37
	PD	68.32	0.65

these peaks slightly shift, as compared with the dehydration peaks of the corresponding cyclodextrins. These results further confirm the formation of PD/CDs complexes, and they are evidence of the inclusion of the PD molecule in the hydrophobic cavities of CDs.

3.6. TG analysis

The thermal properties of the PD/β-CD and PD/γ-CD complexes were investigated using thermogravimetric methods (Fig. S3). A systemic analysis of the TG curves showed that PD decomposes at ca. 273 °C, β-CD at ca. 275 °C and γ-CD at ca. 290 °C. However, the thermal stability of their inclusion complexes differed; that is, the decomposition temperatures were ca. 285 °C and 295 °C for the PD/β-CD and PD/γ-CD complexes, respectively. These results indicate that PD's usual thermal properties were altered after inclusion complexation and that the PD/CD complexes possessed high decomposition temperatures.

XRD and ESI-MS were also used to confirm the structure of the platinum inclusion complex. For analysis details, please see the supporting information (Fig. S1, S2).

3.7. Solubilization

A solubility study was carried out according to a previously reported method [41]. The water solubility of the PD/CD complex was assessed with the preparation of a saturated solution. An excess amount of the complex was placed in 2 mL of water (ca. pH 7.0) and the mixture was stirred for 1 h. After removing the insoluble substance by filtration, the filtrate was evaporated under reduced pressure to dryness and the residue was dosed using the weighing method. The results show that the water solubility of this PD, compared to that of native PD (ca. 0.161 mg/mL) [42], increased remarkably to approximately 7.21 and 12.02 mg/mL through the solubilizing effects of β-CD and γ-CD, respectively. In the control experiment, a clear solution was obtained after dissolving the PD/β-CD 28.17 (mg) and PD/γ-CD 51.98 (mg) complexes, which were equivalent to 7.21 and 12.02 mg/mL of PD, respectively, in 1 mL of water at room temperature. This confirmed the reliability of the satisfactorily obtained water solubility of the PD/CD complex, which will be more conducive for human consumption and absorption as herbal medicine.

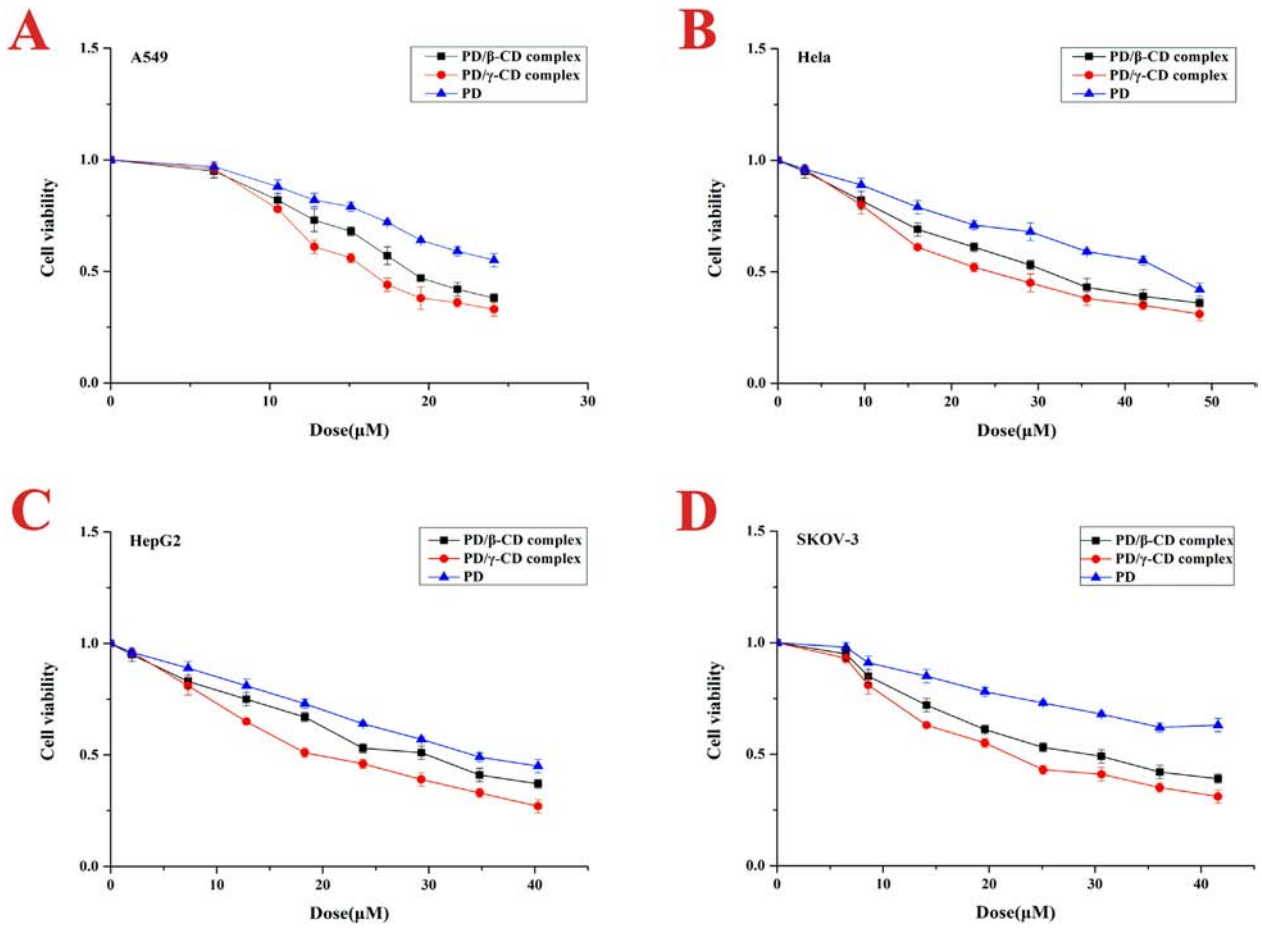

Fig. 5. Exponentially growing cells in 96-well plates were continuously treated with the indicated concentrations of PD for 48 h and then subjected to MTT viability assay. Dose-response curves of PD in (A) A549, (B) Hela, (C)HepG2 and (D) SKOV-3 cells 48 h following treatment.

3.8. Cell growth inhibition assay analysis

The cytotoxicity of PD and its complexes in 4 cancer cell lines was determined by MTT assay [27]. The decrease in absorbance in this assay was due to cell death or reduction in cell proliferation. As shown in Table 2, compared with the published articles [9–11], free PD exhibit broad-spectrum growth inhibition and the similar biological activity against A549, Hela and SKOV-3 cells. However, in this article, the two PD/CD complexes displayed the better cytotoxicity of free PD against A549, Hela, HepG2 and SKOV-3 cells, indicating that, owing to the improved water solubility, the anti-tumour bioavailability of the inclusion complexes also improved.

A dose-dependent inhibition of human cancer cells was shown (Fig. 5). By comparing the effects of PD/CDs complexes in inhibiting cell, it was found that 19.5 μM complexes caused 62% (PD/γ-CD complex), 53% (PD/β-CD complex) and 36% (PD) loss of cell viability in A549 lung cancer cells (Fig. 5A). As shown in Fig. 5 (B, C, D), PD/CDs complexes also caused a better loss of cell viability than PD at the same concentration. The results showed that PD/β-CD and PD/γ-CD have some broad-spectrum anti-tumour activity. Through the report paper [9,11] and the biological activity of complexes, the PD/CDs complexes will be potentially useful for its application as herbal medicine or healthcare products.

4. Conclusions

The inclusion complexation behaviors of PD with β-CD and γ-CD were investigated using SEM, UV–vis, DSC, TG, FT-IR, NMR, XRD and ESI-MS methods. The spectral shifts revealed that the phenyl group of PD is entrapped in the CD's cavity by using continuous variation Job's methods, and 1:1 stoichiometry was confirmed. The 1:1 binding model of complexes were visually proven through the ESI-MS experiment. As the inclusion systems obviously enhanced PD solubility and the dissolution rate, the water solubility of PD was significantly improved from 0.161 mg/mL to 7.21 mg/mL (PD/β-CD complex) and 12.02 mg/mL (PD/γ-CD complex). And the anti-tumour activity against A549, Hela, HepG2 and SKOV-3 cells was also increased. The inclusion complexation technology may be considered a promising approach and an important step in the design of novel formulations of PD as an anticancer therapy or herbal medicine.

Acknowledgments

This work was supported by the Program for Changjiang Scholars and Innovative Research Team in University (No. IRT13095), the National Natural Science Foundation of China (Nos. 21442006, 21262043 and 20902079). The authors thank the High Performance Computing Center at Yunnan University for use of the high performance computing platform.

Appendix A. Supplementary data

Supplementary material that may be helpful in the review process should be prepared and provided as a separate electronic file. That file can then be transformed into PDF format and submitted along with the manuscript and graphic files to the appropriate editorial office. Supplementary data associated with this article can be found in the online version, at http://dx.doi.org/10.1016/j.molliq.2016.03.054

References

[1] R. Brouillard, F. George, A. Fougerousse, Biofactors 6 (1997) 403–410.
[2] X. Wang, R. Song, Y. Chen, M. Zhao, K.S. Zhao, Expert Opin. Investig. Drugs 22 (2013) 169–179.
[3] X. Wang, R. Song, H.N. Bian, U.T. Brunk, M. Zhao, K.S. Zhao, Am. J. Phys. Regul. Integr. Comp. Phys. 302 (2012) R805–R814.
[4] K.S. Zhao, C. Jin, X. Huang, J. Liu, W.S. Yan, Q. Huang, W. Kan, Clin. Hemorheol. Microcirc. 29 (2003) 211–217.
[5] Q. Miao, S. Wang, S. Miao, J. Wang, Y. Xie, Q. Yang, Phytomedicine 19 (2011) 8–12.
[6] Y. Cheng, H.T. Zhang, L. Sun, S. Guo, S. Ouyang, Y. Zhang, J. Xu, Brain Res. 1110 (2006) 193–200.
[7] J.P. Gao, C.X. Chen, W.L. Gu, Q. Wu, Y. Wang, J. Lu, Fitoterapia 81 (2010) 953–960.
[8] U. Indraccolo, F. Barbieri, Eur. J. Obstet. Gynecol. Reprod. Biol. 150 (2010) 76–79.
[9] Y. Zhang, Z. Zhuang, Q. Meng, Y. Jiao, J. Xu, S. Fan, Oncol. Lett. 7 (2014) 295–301.
[10] S.J. Hogg, K. Chitcholtan, W. Hassan, P.H. Sykes, A. Garrill, Obstet. Gynecol. Int. 2015 (2015) 279591.
[11] Y. Wang, J. Ye, J. Li, C. Chen, J. Huang, P. Liu, H. Huang, Cardiovasc. Diabetol. 15 (2016) 19.
[12] G. Murtaza, Acta Pol. Pharm. 69 (2012) 581–590.
[13] Y. Kawabata, K. Wada, M. Nakatani, S. Yamada, S. Onoue, Int. J. Pharm. 420 (2011) 1–10.
[14] M. Liu, A. Chen, Y. Wang, C. Wang, B. Wang, D. Sun, Food Chem. 168 (2015) 270–275.
[15] C. Liu, W. Zhang, H. Yang, W. Sun, X. Gong, J. Zhao, Y. Sun, G. Diao, PLoS One 9 (2014), e101761.
[16] M. Jug, N. Mennini, K.E. Kover, P. Mura, J. Pharm. Biomed. Anal. 91 (2014) 81–91.
[17] J. Szejtli, Chem. Rev. 98 (1998) 1743–1754.
[18] J.Q. Zhang, D. Wu, K.M. Jiang, D. Zhang, X. Zheng, C.P. Wan, H.Y. Zhu, X.G. Xie, Y. Jin, J. Lin, Carbohydr. Res. 406 (2015) 55–64.
[19] J.Q. Zhang, K. Li, Y.W. Cong, S.P. Pu, H.Y. Zhu, X.G. Xie, Y. Jin, J. Lin, Carbohydr. Res. 396 (2014) 54–61.
[20] C.F. Xiao, K. Li, R. Huang, G.J. He, J.Q. Zhang, L. Zhu, Q.Y. Yang, K.M. Jiang, Y. Jin, J. Lin, Carbohydr. Polym. 102 (2014) 297–305.
[21] L.J. Yang, B. Yang, W. Chen, R. Huang, S.J. Yan, J. Lin, J. Agric. Food Chem. 58 (2010) 8545–8552.
[22] S. An, J. He, L. Sun, D. Ren, Y. Ban, J. Mol. Struct. 1037 (2013) 9–14.
[23] B. Liu, Y. Li, H. Xiao, Y. Liu, H. Mo, H. Ma, G. Liang, J. Food, Science 80 (2015) C1156–C1161.
[24] J. Biernacka, K. Betlejewska-Kielak, J. Witowska-Jarosz, E. Klosinska-Szmurlo, A.P. Mazurek, J. Incl. Phenom. Macrocycl. Chem. 78 (2014) 437–443.
[25] W.X. de Paula, A.M. Denadai, M.M. Santoro, A.N. Braga, R.A. Santos, R.D. Sinisterra, Int. J. Pharm. 404 (2011) 116–123.
[27] A. Cutrignelli, A. Lopedota, N. Denora, R.M. Iacobazzi, E. Fanizza, V. Laquintana, M. Perrone, V. Maggi, M. Franco, J. Pharm. Sci. 103 (2014) 3932–3940.
[28] P. Job, Anal. Chim. (1928) 113–203.
[29] P. Guo, Y. Su, Q. Cheng, Q. Pan, H. Li, Carbohydr. Res. 346 (2011) 986–990.
[30] J. Carmichael, W.G. DeGraff, A.F. Gazdar, J.D. Minna, J.B. Mitchell, Cancer Res. 47 (1987) 936–942.
[31] M.T. Faucci, F. Melani, P. Mura, J. Pharm. Biomed. Anal. 23 (2000) 25–31.
[32] H.J. Schneider, F. Hacket, V. Rudiger, H. Ikeda, Chem. Rev. 98 (1998) 1755–1786.
[33] M.V. Rekharsky, R.N. Goldberg, F.P. Schwarz, Y.B. Tewari, P.D. Ross, Y. Yamashoji, Y. Inoue, J. Am. Chem. Soc. 117 (1995) 8830–8840.
[34] A.C. Servais, A. Rousseau, M. Fillet, K. Lomsadze, A. Salgado, J. Crommen, B. Chankvetadze, J. Sep. Sci. 33 (2010) 1617–1624.
[35] E. Bednarek, W. Bocian, J. Poznański, J. Sitkowski, N. Sadlej-Sosnowska, L. Kozerski, J. Chem. Soc. Perkin Trans. 2 (2002) 999–1004.
[36] P. Dandawate, K. Vemuri, K. Venkateswara Swamy, E.M. Khan, M. Sritharan, S. Padhye, Bioorg. Med. Chem. Lett. 24 (2014) 5070–5075.
[37] A. Zoppi, A. Delrivo, V. Aiassa, M. Longhi, AAPS PharmSciTech 14 (2013) 727–735.
[38] M.J. Mora, L.I. Tártara, R. Onnainty, S.D. Palma, M.R. Longhi, G.E. Granero, Carbohydr. Polym. 98 (2013) 380–390.
[39] P.P. Menezes, M.R. Serafini, B.V. Santana, R.S. Nunes, L.J. Quintans Jr., G.F. Silva, I.A. Medeiros, M. Marchioro, B.P. Fraga, M.R.V. Santos, A.A.S. Araújo, Thermochim. Acta 548 (2012) 45–50.
[40] X.H. Wei, S.J. Yang, N. Liang, D.Y. Hu, L.H. Jin, W. Xue, S. Yang, Molecules 18 (2013) 1325–1336.
[41] P. Montassier, D. Duchêne, M.C. Poelman, Int. J. Pharm. 153 (1997) 199–209.
[42] K. Schulze, L. Schreiber, I. Szankowski, J. Agric. Food Chem. 53 (2005) 356–362.